Earth and Planetary Science Letters 309 (2011) 153–165

Contents lists available at ScienceDirect

Earth and Planetary Science Letters

journal homepage: www.elsevier.com/locate/epsl

# Paleomagnetism of early Paleogene marine sediments in southern Tibet, China: Implications to onset of the India–Asia collision and size of Greater India

Zhiyu Yi *, Baochun Huang, Junshan Chen, Liwei Chen, Hailong Wang

*State Key Laboratory of Lithospheric Evolution, Institute of Geology and Geophysics of the Chinese Academy of Sciences, Beijing 100029, China*

ARTICLE INFO

*Article history:*
Received 10 March 2011
Received in revised form 30 June 2011
Accepted 1 July 2011
Available online 28 July 2011

Editor: T.M. Harrison

*Keywords:*
Tethyan Himalaya
Greater India
India–Asia collision
paleomagnetism
Paleogene
marine sediments

ABSTRACT

We report a paleomagnetic study of Paleocene marine sediments in the Gamba area of the Tethyan Himalayan terrane, southern Tibet, which aims to accurately locate the position of the northern margin of Greater India and further constrain timing of initial contact between India and Asia. Following detailed rock magnetic and paleomagnetic experiments on a total of 675 drill-core samples collected from the Zongpu and Upper Jidula formations, characteristic remanent magnetizations (ChRMs) were successfully isolated from most samples following alternating field (AF) or integrated thermal and AF demagnetization. The ChRMs are of dual polarity and pass fold and reversal tests indicating a pre-folding origin. Together with detailed biostratigraphic investigation of the sampling section, a magnetic polarity sequence is constructed from data at 167 sampled horizons and satisfactorily correlates with polarity chrons C24r to C27r dating the Zongpu Formation between ~56.2 and 61.8 Ma on the geomagnetic polarity time scale. The ChRM directions from the Zongpu Formation are grouped stratigraphically into 33 sites and yield two paleopoles of 71.6°N, 277.8°E ($A_{95}=2.5°$) and 67.3°N, 266.3°E ($A_{95}=3.5°$) for the time intervals comprising 56 to 59 Ma and 59 to 62 Ma, respectively. These new paleopoles imply that the Tethyan Himalayan terrane was sited at low latitudes in the Northern Hemisphere during the interval ~62–56 Ma, suggesting that initial contact between the Tethyan Himalaya and Lhasa terranes was established before 60.5 ± 1.5 Ma, and very likely occurred near the Cretaceous–Tertiary boundary, at least in the central part of the suture zone. The results also indicate that at least 1500 ± 480 km of post-collisional crustal shortening occurred within the Himalayas. From the analysis of available paleomagnetic data obtained on both sides of the suture zone, we propose a conceptional collision model for the India–Asia collision.



## 1. Introduction

Collision of India and Asia has created the Tibetan plateau (Allègre et al., 1984; Chang et al., 1986; Dewey et al., 1989), and the continuous evolution of the Tibetan plateau has greatly changed the environment in surrounding areas (Brookfield, 1998; Clark et al., 2004; Molnar et al., 1993; Raymo and Ruddiman, 1992). The initial time of the India–Asia collision is undoubtedly one of the most important boundary conditions for the evolution model of the Himalaya–Tibetan orogenic system, and thus becomes a starting point for almost all studies in the Tibetan plateau (Chen et al., 2010).

The timing of collision between India and Asia has been a controversial issue during the past decade and several recent paleomagnetic studies have aimed to constrain the latitudinal position of the initial contact between India and Asia (e.g., Chen et al., 2010; Dupont-Nivet et al., 2010; Liebke et al., 2010; Najman et al., 2010). These investigations have ruled out the model for an Oligocene India–Asia collision (e.g., Aitchison et al., 2000, 2007; Aitchison and Davis, 2001; Ali and Aitchison, 2008), and implied that initial contact between India and Asia occurred no later than ~50 Ma (Chen et al., 2010; Dupont-Nivet et al., 2010; Liebke et al., 2010; Najman et al., 2010). Although these studies strongly support the traditional view of the timing India–Asia collision at ~55–50 Ma (e.g., Klootwijk et al., 1992; Patriat and Achache, 1984), the model for a much earlier collision, for example during the late Cretaceous or near the Cretaceous–Paleogene (K/Pg) boundary (e.g., Cai et al., 2011; Ding et al., 2003, 2005; Jaeger et al., 1989; Mo et al., 2003, 2008) still retain support. Collision between two continents is defined as the contact between continental lithospheres accompanied by the disappearance of oceanic lithosphere. Therefore, for a continental collision in approximately a north–south direction as in the India–Asia collision, the most direct evidence is whether terranes distributed in both sides of suture zone have comparable paleolatitudes. This provides the key evidence for understanding when and where the Indian and Asian continents initially collided (Huang et al., 2010).

Recently, several paleomagnetic studies have been carried out on the Linzizong volcanic rocks in the Lhasa terrane (Chen et al., 2010; Dupont-Nivet et al., 2010; Liebke et al., 2010; Sun et al., 2010; Tan et al., 2010) and group-mean results for individual formation indicate

* Corresponding author at: Institute of Geology and Geophysics, Chinese Academy of Sciences, No. 19, Bei Tucheng Xilu, Chaoyang District, Beijing 10029, China. Tel.: +86 10 82998425; fax: +86 10 62010846.
*E-mail addresses:* yizhiyu09@gmail.com (Z. Yi), bchuang@mail.iggcas.ac.cn (B. Huang).

0012-821X/$ – see front matter © 2011 Elsevier B.V. All rights reserved.
doi:10.1016/j.epsl.2011.07.001

that the leading edge of the Asian continent was located at 6.7°N for the Dianzhong, 11.6°N for the Nianbo, and 16.8°N for the Pana formations (Najman et al., 2010). Our newly revised paleomagnetic data for the Linzizong Group in the Linzhou basin of the Lhasa terrane (Fig. 1a) yield three individual paleopoles at 66.4°N, 262.5°E (N = 20, $A_{95}$ = 6.3°), 69.7°N, 268.6°E (N = 13, $A_{95}$ = 6.3°), and 68.6°N, 232.3°E (N = 18, $A_{95}$ = 5.9°) for the Dianzhong (~64–60 Ma), Nianbo (~60–50 Ma), and Pana formations(~50–44 Ma), respectively (Chen et al., in progress). Collectively, these data indicate low paleolatitudes of 5.8°N ± 6.3° to 11.5°N ± 5.9° for the Lhasa terrane during formation of the Linzizong Group.

However, late Cretaceous to early Paleogene paleomagnetic data obtained from the Himalayan terrane, which lies on the southern side of the Indus–Yarlung Zangbo suture zone (IYSZ, Fig. 1a), are still rare because of poor natural conditions, serious remagnetization and the lack of volcanic rocks. The paucity of reliable paleomagnetic data with precise age constraints in the Tethyan Himalaya is obviously unfavorable for determination of the shape and size of Greater India and for defining the paleogeographic position of the northern leading edge of the Indian continent. To address this problem, some researchers have attempted to use paleolatitudes calculated from remagnetization components in older rocks on the assumption that they were acquired during the India–Asia collision (e.g., Appel et al., 1991, 1995; Tong et al., 2008). Nevertheless, uncertainties about the timing and orientation of these remagnetizations, as well as relative poor quality of definition of the remagnetization component data themselves, make this kind of endeavor poorly effective. Besse et al. (1984) reported a paleomagnetic result from the Paleocene Himalayan sediments in the Dingri area (Table S1), but this preliminary result has been repeatedly criticized due to the few available sampling sites (e.g. Liebke et al., 2010) and imprecise age of the sampled strata (Jaeger et al., 1989). On the other hand, Patzelt et al. (1996) preformed an encouraging paleomagnetic study on late Maastrichtian to Paleocene marine sediments in the Gamba and Duela areas of southern Tibet where some primary remanences were found to be well-preserved in late Cretaceous to early Paleogene marine depositions. The results yielded low paleolatitudes of 4.7°S ± 4.4° and 5.0°N ± 3.8° for the northern edge of Greater India (reference site: 29.3°N, 88.5°E) during late Maastrichtian and Paleocene times, respectively. An Elongation/Inclination (E/I) analysis (Tauxe, 2005) on these data identified little or no apparent inclination-shallowing (Dupont-Nivet et al., 2010). Further comparison of these paleopoles indicates a poleward transport of 9.6° ± 4.7° during the interval between deposition of the Zongshan and Zongpu formations and

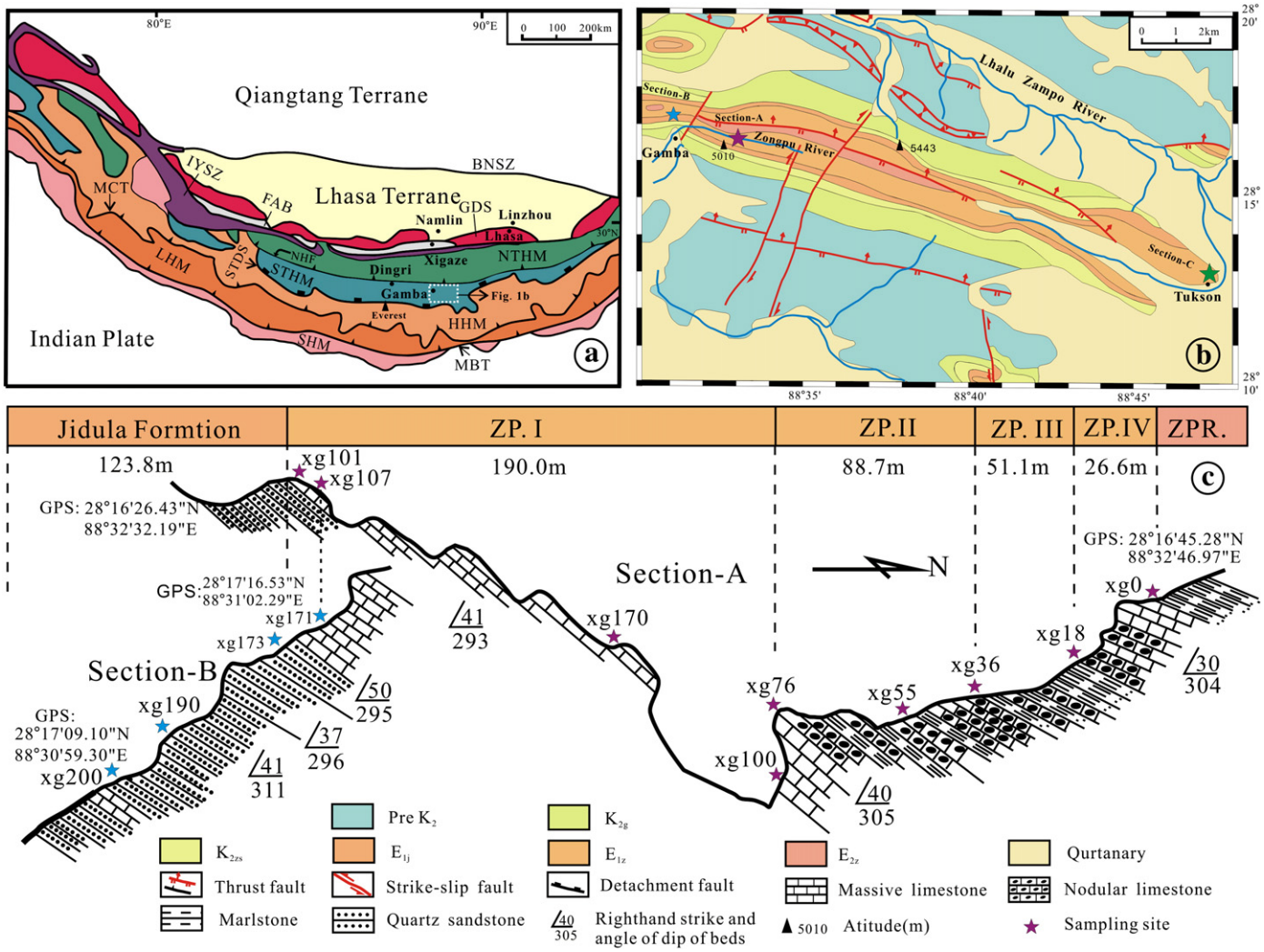


**Fig. 1.** (a) Schematic map of the India–Asia collision zone modified after Gansser (1964) showing main petrologic and tectonic units of the Himalayas and the Lhasa terrane. IYSZ, Indus–Yarlung Zangbo suture (ophiolite belt); GDS, Gangdise arc (granite belt); FAB, forearc basin (flysch belt); NTHM, North Tethyan Himalayan zone; STHM, South Tethyan Himalayan zone; HHM, Higher Himalaya (crystalline rocks); LHM, Lesser Himalaya; SHM, Sub-Himalaya; MBT, Main Boundary thrust; MCT, Main Central thrust; STDS, South Tibetan detachment system; NHF, North Himalayan fault; BNSZ, Bangong–Nujiang suture. (b) Simplified geologic map of the Gamba area showing Meso-Cenozoic stratigraphy and paleomagnetic sampling locations. (c) Composite cross section of the sedimentary succession exposed in the Gamba area showing major stratified units and distribution of sampling sites. ZP and ZPR represent the Zongpu and Zhepure formations, respectively.

provides a first-order paleomagnetic constraint on the shape of Greater India and onset of the India–Asia collision. However, due to fast northward movement of the Himalayan terrane during late Maastrichtian to Paleocene times, these preliminary results are obviously not enough to define motion details for the Himalayan terrane during this period, and are insufficient to accurately determine the timing of India–Asia collision as well as potential collision-related crustal shortening within the Himalayas. Therefore, more combined paleontostratigraphic and paleomagnetic investigations on late Cretaceous–Paleogene marine successions in the Himalayas are required to resolve these issues (Chen et al., 2010).

In this study, we carry out a combined magnetostratigraphic and magnetotectonic study of early Paleogene Tethyan marine sediments in the Gamba area of southern Tibet, where relatively detailed paleontostratigraphic investigations (Wan et al., 2002a, b; Willems and Zhang, 1993) and the potential preservation of primary remanence (Patzelt et al., 1996) provide a sound basis for our study. We thereby aim to obtain some early Paleogene paleopoles with precise age constraints and accurately locate the northern leading edge of the Indian continent. Together with recently-obtained paleomagnetic constraints from the southern leading edge of the Asian continent, this enables us to estimate the timing of initial contact between India and Asia, the northern extension of Greater India, and to further develop a geodynamic model for the India–Asia collision.

## 2. Geological setting and paleomagnetic sampling

The structure of the India–Asia collision orogenic belt is shown in Fig. 1a, in which primary tectonic units from north to south comprise the Lhasa terrane, the IYSZ, and the Himalayan terrane. The later is generally regarded as the northern part of the Indian plate where a complex fold–fault system developed during the convergence and collision of India and Asia (e.g. Yin and Harrison, 2000). The main tectonic boundaries within the Himalayas consist of the South Tibetan detachment system (STDS), Main Central thrust (MCT), Main Boundary thrust (MBT), which accordingly divided the Himalayas into the Tethyan Himalaya, Higher Himalaya, Lesser Himalaya and Sub-Himalaya. The Tethyan Himalaya can be further divided into North and South zones by the Tingri–Gamba Fault which regionally belongs to the North Himalayan Fault (NHF). The North Tethyan Himalaya zone is built up mainly of limestones, cherts, sandstones and mélanges representative of a sedimentary assemblage formed in shelf slope to deep basin environments. The South Zone is built up mainly of limestones, well-sorted sandstones and marls indicative of a stable shelf environment (e.g., Pan and Ding, 2005). Noting that the shelf slope to deep basin environments generally marks the transition between continental and oceanic crusts (Hedberg, 1970), and that crustal shortening in the Tethyan Himalaya has been estimated to be only ~130–140 km (Ratschbacher et al., 1994), it is possible that the Tethyan Himalaya is preserved as the northern leading edge of Greater India.

In the Gamba area, a continuous late Cretaceous to early Paleogene marine sedimentary succession is well-preserved as three lithostratigraphic units namely the Zongshan, Jidula and Zongpu formations (Gansser, 1964; Wan et al., 2000, 2002a,b; Wen, 1987a,b; Willems and Zhang, 1993). Detailed lithological and biostratigraphic studies are given by Wan (1985); Willems and Zhang (1993) and Wan et al. (2000, 2002a,b). The Jidula Formation consists mainly of ferruginous sandstones with a thickness of ~130 m which can be sub-divided into three members comprising lower sandstones (Member I), black limestones (Member II), and upper sandstones (Member III). Appearance of the foraminifera *Rotalia hensoni* Smout, *R. dukharni* Smout, *Smoutina cruysi* Drooger, *Lockhartia* sp. along with *Rotalia* sp. and *Smoutina* sp. at the bottom of the Jidula Formation indicate a Danian age (Wan et al., 2002a). The Zongpu Formation is mainly composed of carbonate rocks with a thickness of ~360 m and could be sub-divided into four members comprising, in ascending order, massive limestones (Member I), marls (Member II), nodular limestones (Member III), and well-bedded limestones (Member IV). Planktonic foraminifera of the *angulata* zone occurring at 5.5 m above the base of this formation suggest that the Member I is to be classified into the Middle Paleocene. This is confirmed by ostracods appearing in the lower part of Member I (about 4.5 m above the boundary) which suggest a Danian age; the more frequent occurrence of foraminifera *Miscellanea miscella* for the first time at the top of the Member I indicates a Thanetian age. Strata developed from the top of Member I to the top of the Member III have a clear Thanetian age in the light of the predominant distribution of *Miscellanea miscella*, *Discocyclina* and *Ranikothalia*. The expansion of the foraminifera genus *Alveolina, Orbitolites* and first small *Nummulites* permits an assignment of the upper ~25 m of the Zongpu Formation to Eocene time (Willems and Zhang, 1993).

Our sampling area near the town of Gamba is shown in Fig. 1b, where a relatively complete succession of the Zongpu Formation was selected for magnetostratigraphic sampling. Three or more individually oriented drill-cores were collected from each horizon with a sampling interval typically of 1–2 m between successive horizons, although it was sometimes as large as 3–5 m or more where the sequence was composed mostly of marls. A total of 510 samples were collected from 170 horizons comprising a total sampling thickness of ~356.4 m (Fig. 1c). Meanwhile, type section of the Jidula Formation developed near the town of Gamba was also sampled although only 84 cores of sandstone in 30 horizons were collected because of incomplete development of the succession and the prevalence of coarse grain sizes (Fig. 1b–c). A further 81 samples from 8 sites of well-bedded limestones, belonging lithologically to Member I of the Zongpu Formation were collected for a fold test from the section near the village of Tukson, about several tens kilometers away from the type section of the Zongpu Formation (Fig. 1b). All the samples were collected with a portable gasoline-powered drill and oriented in situ by both magnetic and sun compasses.

## 3. Rock magnetic investigations

Cylindrical specimens ~2.0–2.2 cm in length were cut from field core samples and some selected fresh end materials were subjected to rock magnetic analysis. Acquisition and back-field demagnetization of isothermal remanent magnetization (IRM) as well as thermal demagnetization of composite IRMs (Lowrie, 1990), were carried out to identify the main magnetic minerals in the collected samples. Twelve pilot samples were magnetized with a pulse magnetizer (2G660) from 0.01 to 2.4 Tesla (T), and IRM intensity measured following each step of magnetization. After executing back-field demagnetization of IRM, direct current (DC) magnetic fields of 2.7, 0.4 and 0.1 T were applied to the Z-axis, Y-axis and X-axis of each sample separately. Thermal demagnetization up to 680 °C was performed in a TD-48 thermal demagnetizer and remanent magnetizations were measured using a 2G-755R cryogenic magnetometer.

The samples can be divided into three categories according to results of rock magnetic experiments. Firstly, most limestone samples from the Zongpu Formation reveal a complete saturation at ~0.3 T with remanence coercivity (Hcr) less than 0.1 T (Fig. S1a). This indicates that these samples are dominated by low-coercivity ferromagnets. Similarly demagnetization of composite IRMs indicates that all three components decreased dramatically at ~400°C and the soft and medium components unblock completely at ~480°C (Fig. S1e) significantly below the Curie point of pure magnetite. A few limestone samples from the Zongpu Formation and most sandstone samples from the Jidula Formation show a rapid increase in IRM intensity before 0.2 T and a further gradual increase up to 2.4 T, the remanence coercivity generally lies between 0.1 and 0.2 T (Fig. S1b–c), suggesting that these samples are composed of both low and high coercivity magnetic minerals. Demagnetization of the composite IRMs shows that the hard and medium components usually unblock completely at 650 °C indicative of the presence of hematite; the dramatic decrease of IRM intensity of the soft and medium components at ~400 °C, as well as the complete unblocking of the soft component at ~500 °C to 560 °C (Fig. S1f–g), identifies the

presence of magnetite. A few limestone samples from the Zongpu Formation show a very slow increase of IRM intensity before 0.5 T and fail to saturate up to 2.4 T with higher remanence coercivity in excess of ~0.5–1.0 T (Fig. S1d). Demagnetization of composite IRMs indicated that the hard component was generally unblocked during temperature intervals between 80 and 200 °C (Fig. S1h) indicating that these samples are dominated by goethite.

Collectively, the main magnetic carriers of remanence are either magnetite in most limestones from the Zongpu Formation, or both magnetite and hematite in some limestones from the Zongpu Formation and in sandstones from the Jidula Formation; goethite appears to predominate in a few limestone and sandstone samples.

## 4. Paleomagnetic results and analysis

Following evaluation of rock magnetic behaviors resolved from pilot samples, all specimens were subject to either progressive thermal or AF demagnetization. In general, progressive AF demagnetization or an integrated approach comprising thermal demagnetization to 250 °C followed by AF demagnetization up to 89 mT was applied to specimens from the Zongpu Formation in the light of their relatively lower natural remanent magnetization (NRM) (generally less than 0.1 mA/m) and the predominance of low-coercivity magnetic minerals. For the specimens from the Jidula Formation, however, only thermal demagnetization was applied because of the existence of high-coercivity hematite. Thermal demagnetization was performed in a TD-48 thermal demagnetizer with residual magnetic field minimized to less than 10 nT inside the cooling chamber. Demagnetization intervals were 50 or 100 to 500 °C, subsequently reduced to steps of 30, 20 or 10 °C as the maximum unblocking temperatures of the remanence carriers were approached. Magnetizations were measured using a 2G-755R cryogenic magnetometer and performed in the Paleomagnetism and Geochronology Laboratory (PGL) of the Institute of Geology and Geophysics, Chinese Academy of Sciences where magnetometers and demagnetizers are installed in a magnetic shielded room with the field minimized to less than 300 nT. Demagnetization results were evaluated using stereographic projections and orthogonal (Zijderveld, 1967) diagrams with the latter used to resolve component structures. Equivalent component directions were calculated by principal component analysis (Kirschvink, 1980) or great-circle fitting of magnetizations (McFadden and McElhinny, 1988), and interval-mean results were determined using standard Fisherian method (Fisher, 1953).

In general, for the specimens from the Zongpu Formation, a soft viscous component or a low temperature component with an in-situ direction approximately paralleling the present geomagnetic field is removed by about 15 mT or 250 °C. After this removal, 284 out of 510

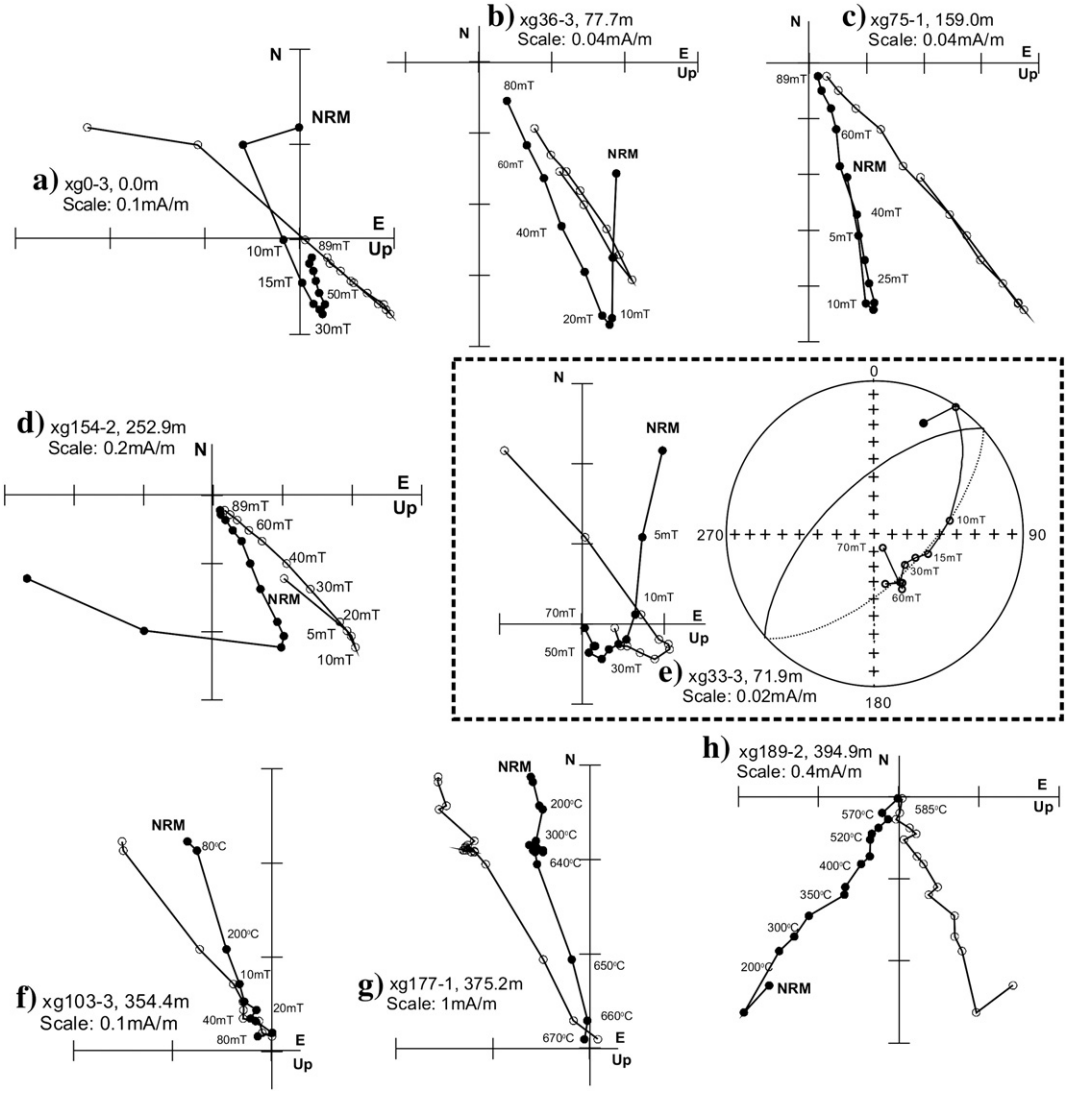


**Fig. 2.** Orthogonal (Zijderveld) and stereonet vector plots of representative specimens from different levels. Directions are plotted in-situ; solid and open circles represent vector endpoints projected onto horizontal and vertical planes (lower and upper hemisphere), respectively.

specimens yield a well defined characteristic remanence (ChRM) recognized by at least four successive steps between 20 and 89 mT (Fig. 2a–d, f) and with maximum angular deviation (MAD) less than 10°. On the other hand, there are 35 out of the remaining 226 specimens showing a clear distribution of NRM endpoints along a great circle, indicating that the ChRM may have been obliterated (Fig. 2e); in these cases some interval-mean directions of ChRM were calculated by combining remagnetization great circles with direction observations using McFadden and McElhinny's (1988) method. However, the other remaining 191 demagnetized specimens did not yield any stable ChRM after the removal of a viscous component and the scattered NRM directions on equal-area projection diagrams during demagnetization indicated a poor record of the paleomagnetic field.

For the Jidula Formation, only 20 out of 84 demagnetized specimens yielded a stable high temperature ChRM after the removal of a viscous component by temperatures of 250–300 °C. The ChRM is generally isolated over the temperature intervals of either 610–670 °C or 500–590 °C (Fig. 2g–h). This demagnetization behavior is compatible with the rock magnetic results which identify the presence of both magnetite and hematite. Unfortunately, most specimens yielded erratic demagnetization trajectories and failed to isolate a ChRM component. We have no concise explanation for this behavior but it does seem to correlate with the relatively coarse grain-sizes of sandstone specimens. The 20 ChRM directions are predominantly of reversed polarity and yield an interval-mean of $D=198.8°$, $I=-28.3°$, $\alpha_{95}=8.1°$ before and $D=200.4°$, $I=4.1°$, $\alpha_{95}=7.4°$ after tilt correction with slight improvement of the data grouping (Fig. 3a–b).

A total of 167 out of 200 sampled horizons from the Zongpu and Jidula formations yielded well-defined ChRMs clustering within 40° of the mean in a NW-to-NE quadrant with moderate inclinations and the equivalent antipodes and MAD values of less than 15° (Table S2 and Fig. S2a). The reversal test (McFadden and McElhinny, 1990) is positive with an angular difference of 2.0° between tilt-adjusted directions of each polarity. This is less than the critical angle of 10.0° and yields a B class reversal test result. The 339 ChRM directions are grouped stratigraphically into 33 sites, each with an average thickness of ~10 m and typically incorporating 3 to 5 sampling horizons (Table 1). The interval-mean ChRM direction of 14 sites from the upper Zongpu Formation (Member II, III and IV) is $D=163.7°$, $I=-41.2°$ with $\alpha_{95}=3.4°$ before and $D=177.0°$, $I=-19.6°$ with $\alpha_{95}=3.5°$ after tilt correction (Fig. 3c–d); whereas the 18 sites from the lower Zongpu Formation (Member I) yield an interval-mean of $D=169.2°$, $I=-44.3°$ with $\alpha_{95}=4.3°$ before and $D=180.8°$, $I=-11.1°$ with $\alpha_{95}=4.2°$ after tilt correction (Fig. 3e–f).

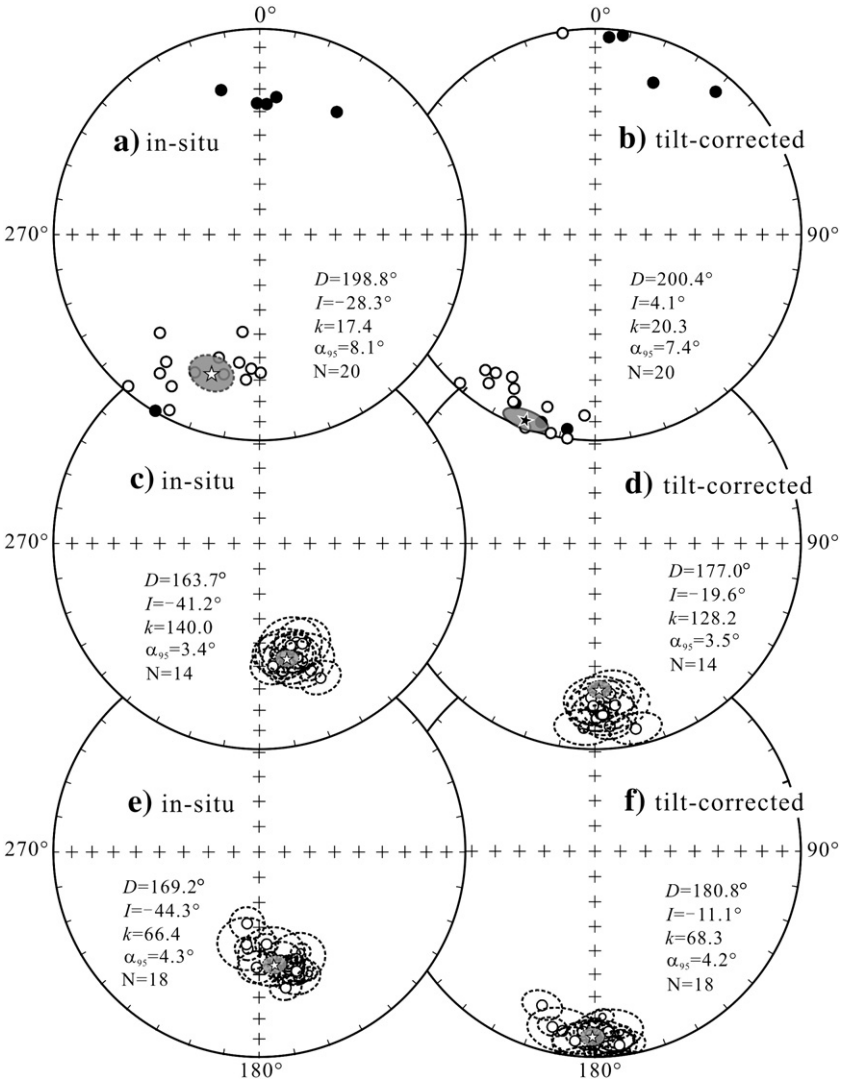


**Fig. 3.** Equal-area projections of the ChRMs before and after tilt adjustment for (a, b) the Jidula quartz sandstones (formation mean values are calculated at the specimen level), (c, d) the upper part (members II, III and IV), and (e, f) the lower part (Member I) of the Zongpu Formation (group means come from the section A only). Solid/open symbols represent downward/upward inclinations; stars indicate the overall mean directions with 95% confidence limits.

**Table 1**
Summary of interval-mean directions and VGPs of ChRMs from the Zongpu and Jidula formations, Southern Tibet.

| Site ID | Depth (m) | Strike/dip | n/n0 | N/R | Dg (°) | Ig (°) | Ds (°) | Is (°) | $k_g/k_s$ | $\alpha_{95}$ g/$\alpha_{95}$ s (°) | Plong (°) | Plat (°) |
|---|---|---|---|---|---|---|---|---|---|---|---|---|
| *Zongpuxi profile(upper part of the section A), Member II + III + IV of the Zongpu Formation, Gamba* | | | | | | | | | | | | |
| ZP1 | 0.0–5.7 | 315/30 | 8/21 | 0/8 | 163.6 | −45.7 | 181.4 | −25.9 | 67.3/73.6 | 6.8/6.5 | 83.1 | −75.3 |
| ZP2 | 8.8–11.7 | 310/29 | 12/21 | 0/12 | 160.0 | −38.9 | 172.9 | −21.8 | 15.0/15.7 | 11.6/11.3 | 111.3 | −71.8 |
| ZP3 | 12.8–21.9 | 307/29 | 13/20 | 0/13 | 167.9 | −39.4 | 179.5 | −16.0 | 45.7/44.3 | 6.2/6.3 | 89.9 | −69.9 |
| ZP4 | 23.8–33.8 | 299/30 | 10/13 | 2/8 | 167.3 | −44.1 | 178.2 | −20.4 | 22.1/20.2 | 10.5/11.0 | 94.3 | −72.2 |
| ZP5 | 34.8–60.2 | 301/26 | 10/29 | 3/7 | 169.7 | −36.9 | 177.4 | −17.6 | 529.7/482.7 | 2.1/2.2 | 96.2 | −70.6 |
| ZP6 | 63.0–75.9 | 293/26 | 10/19 | 0/10 | 171.9 | −44.8 | 180.6 | −22.1 | 35.7/34.8 | 8.2/8.3 | 86.5 | −73.2 |
| ZP7 | 77.7–83.7 | 304/27 | 10/13 | 0/10 | 159.5 | −47.4 | 175.2 | −28.5 | 90.7/90.7 | 5.1/5.1 | 108.2 | −76.2 |
| ZP8 | 85.1–89.1 | 307/29 | 8/9 | 0/8 | 156.8 | −46.0 | 174.2 | −27.5 | 29.3/29.3 | 10.4/10.4 | 111.1 | −75.3 |
| ZP9 | 91.2–94.8 | 304/31 | 9/9 | 0/9 | 164.6 | −41.1 | 177.0 | −18.1 | 24.5/24.5 | 10.6/10.6 | 97.5 | −70.8 |
| ZP10 | 96.4–104.2 | 304/31 | 9/12 | 0/9 | 163.0 | −47.0 | 178.6 | −24.0 | 20.7/20.7 | 11.6/11.6 | 93.5 | −74.2 |
| ZP11 | 105.3–117.7 | 304/32 | 11/17 | 0/11 | 173.7 | −39.8 | 183.5 | −11.2 | 33.5/26.7 | 8.0/9.0 | 79.5 | −67.1 |
| ZP12 | 121.9–127.0 | 307/39 | 9/13 | 0/9 | 155.6 | −29.0 | 167.6 | −8.6 | 52.1/43.4 | 7.2/7.9 | 116.9 | −63.3 |
| ZP13 | 128.6–145.8 | 320/39 | 14/24 | 0/14 | 158.0 | −33.8 | 177.2 | −19.7 | 86.4/82.5 | 4.3/4.4 | 97.3 | −71.7 |
| ZP14 | 147.6–163.7 | 295/44 | 8/18 | 0/8 | 161.5 | −41.3 | 175.4 | −11.9 | 69.9/68.3 | 6.7/6.7 | 100.4 | −67.3 |
| Sub-mean | | | 14/14 | 0/14 | 163.7 | −41.2 | 177.0 | −19.6 | 140.0/128.2 | 3.4/3.5 | 277.8 | 71.6 |
| | | | | | | | | | | | K = 249.8 | $A_{95}$ = 2.5 |
| *Zongpuxi profile (lower part of the section A), Member I of the Zongpu Formation, Gamba* | | | | | | | | | | | | |
| ZP15 | 166.4–169.5 | 307/38 | 10/10 | 0/10 | 165.9 | −40.8 | 179.8 | −12.9 | 72.8/72.8 | 5.7/5.7 | 89.0 | −68.2 |
| ZP16 | 170.8–175.3 | 302/41 | 9/10 | 0/9 | 170.2 | −35.9 | 179.2 | −2.6 | 424.8/175.2 | 2.5/3.9 | 90.3 | −63.0 |
| ZP17 | 177.6–182.1 | 307/38 | 10/12 | 0/10 | 162.8 | −38.9 | 176.7 | −12.4 | 139.7/139.7 | 4.1/4.1 | 97.2 | −67.8 |
| ZP18 | 183.4–189.3 | 307/38 | 8/9 | 0/8 | 157.7 | −36.2 | 171.8 | −12.2 | 365.6/341.7 | 2.9/3.0 | 109.4 | −66.5 |
| ZP19 | 191.1–194.9 | 307/38 | 9/9 | 0/9 | 165.4 | −43.3 | 180.7 | −15.2 | 230.1/230.1 | 3.4/3.4 | 86.5 | −69.4 |
| ZP20 | 197.0–202.6 | 307/38 | 10/12 | 0/10 | 162.9 | −44.7 | 179.9 | −17.3 | 583.8/583.8 | 2.0/2.0 | 88.8 | −70.6 |
| ZP21 | 204.9–212.1 | 307/38 | 13/15 | 0/13 | 157.6 | −46.1 | 177.4 | −20.5 | 124.5/124.3 | 3.7/3.7 | 96.9 | −72.1 |
| ZP22 | 215.1–227.6 | 299/40 | 8/10 | 0/8 | 168.8 | −45.4 | 181.4 | −11.5 | 52.7/54.1 | 7.7/7.6 | 84.9 | −67.5 |
| ZP23 | 232.6–246.5 | 299/40 | 8/13 | 0/8 | 160.8 | −44.2 | 175.7 | −13.1 | 27.7/27.7 | 10.7/10.7 | 99.9 | −68.0 |
| ZP24 | 248.6–256.3 | 299/40 | 8/12 | 0/8 | 162.3 | −36.3 | 172.8 | −5.6 | 54.1/54.1 | 7.6/7.6 | 104.9 | −63.6 |
| ZP25 | 257.8–263.8 | 299/40 | 9/13 | 0/9 | 162.8 | −38.9 | 174.5 | −7.7 | 74.6/74.6 | 6.0/6.0 | 101.6 | −65.0 |
| ZP26 | 271.8–274.4 | 299/40 | 9/10 | 0/9 | 189.6 | −60.8 | 198.9 | −21.9 | 61.8/60.0 | 6.6/6.7 | 38.5 | −65.5 |
| ZP27 | 276.7–283.0 | 294/38 | 9/12 | 0/9 | 186.8 | −50.5 | 193.6 | −13.2 | 116/126.2 | 4.8/4.6 | 55.2 | −64.8 |
| ZP28 | 285.1–288.2 | 289/36 | 8/9 | 0/8 | 181.3 | −42.9 | 186.0 | −8.1 | 65.4/65.4 | 6.9/6.9 | 74.2 | −65.1 |
| ZP29 | 289.8–295.0 | 287/41 | 10/12 | 0/10 | 175.6 | −52.6 | 183.8 | −13.2 | 127.1/127.1 | 4.3/4.3 | 78.3 | −68.1 |
| ZP30 | 296.5–302.8 | 284/40 | 10/13 | 0/10 | 187.9 | −52.3 | 190.2 | −12.3 | 20.6/20.2 | 10.9/11.0 | 63.0 | −65.9 |
| ZP31 | 304.5–321.4 | 290/42 | 12/32 | 0/12 | 173.4 | −47.0 | 180.0 | −6.6 | 13.2/13.2 | 12.4/12.4 | 88.5 | −65.0 |
| ZP32* | 324.9–340.6 | 289/42 | No meaningful interval-mean direction could be isolated | | | | | | | | | |
| ZP33 | 342.3–356.4 | 282/44 | 11/34 | 4/7 | 169.1 | −32.9 | 173.3 | 7.7 | 69.9/81.1 | 5.5/5.1 | 100.9 | −57.2 |
| Sub-mean | | | 18/19 | 0/18 | 169.2 | −44.3 | 180.8 | −11.1 | 66.4/68.3 | 4.3/4.2 | 266.3 | 67.3 |
| | | | | | | | | | | | K = 101.1 | $A_{95}$ = 3.5 |
| *Tukson profile (section C), Member I of the Zongpu Formation, Tukson; used for fold test only* | | | | | | | | | | | | |
| XG277 | | 86/37 | 7/10 | 0/7 | 191.8 | 25.1 | 190.5 | −10.8 | 23.5/23.5 | 12.7/12.7 | | |
| XG278 | | 75/39 | No meaningful site-mean direction could be isolated | | | | | | | | | |
| XG279 | | 77/36 | 9/11 | 0/9 | 209.6 | 38.8 | 199.3 | 9.8 | 33.7/33.7 | 9.0/9.0 | | |
| XG280 | | 67/39 | 7/10 | 0/7 | 202.7 | 25.6 | 197.3 | −3.5 | 12.3/12.3 | 17.9/17.9 | | |
| XG281 | | 86/47 | 6/11 | 0/6 | 210.1 | 32.3 | 204.6 | −8.5 | 78.7/78.7 | 7.6/7.6 | | |
| XG282 | | 89/41 | 6/11 | 0/6 | 205.8 | 21.4 | 204.8 | −15.6 | 18.1/18.1 | 16.2/16.2 | | |
| XG283 | | 66/37 | No meaningful site-mean direction could be isolated | | | | | | | | | |
| XG284 | | 72/47 | No meaningful site-mean direction could be isolated | | | | | | | | | |
| Sub-mean | | | 5/8 | 0/5 | 203.8 | 28.8 | 199.3 | −5.8 | 72.7/51.4 | 9.0/10.8 | | |
| Group-mean for Member I | | | 23/24 | 0/23 | 177.8 | −31.3 | 184.8 | −10.1 | 5.9/40.8 | 13.7/4.8 | | |
| Jidula profile (section B), upper part of the Jidula Formation, Gamba | | | | | | | | | | | | |
| XG173-200 | 366.0–430.2 | 56/35 | 20/84 | 5/15 | 198.8 | −28.3 | 200.4 | 4.1 | 17.4/20.3 | 8.1/7.4 | 232.3 | 53.9 |
| | | | | | | | | | | | dp/dm = 3.7/7.4 | |

Abbreviations are: site ID, Site identification; Depth, vertical distance between grouped site and upper boundary of the Zongpu Formation; Strike/dip, strike azimuth and dip of bed; $n/n_0$, number of samples or sites demagnetized or used to calculate or yield well-defined ChRMs; N/R, samples or sites showing normal/reversed polarity; Dg and Ig, $\kappa_g$, $\alpha_{95g}$ (Ds and Is, $\kappa_s$, $\alpha_{95s}$), declination and inclination of direction, precision parameter, 95% confidence limit of Fisher statistics in-situ (after tilt adjustment). Plong and Plat are longitude and latitude of corresponding virtual geomagnetic pole (VGP) in stratigraphic coordinates.

In addition, five out of eight sampled sites from section C, which have contrasting tectonic orientation from sections A and B and were collected specifically for the purpose of applying a fold test, also yield stable ChRMs following removal of a viscous overprint. Demagnetization characteristics of these specimens are often similar to limestone specimens from the Zongpu Formation in section A; these specimens show only reversed polarity. The overall group-mean direction of the total of 23 sites from Member I of the Zongpu Formation (both sections A and C) is $D = 177.8°$, $I = -31.3°$ with $\alpha_{95} = 13.7°$ before and $D = 184.8°$, $I = -10.1°$ with $\alpha_{95} = 4.8°$ after tilt correction. The data grouping is significantly improved by tilt adjustment with $k_s/k_g = 6.9$ (Fig. 4a–b). Application of McFadden's (1990) fold test indicates a positive result at 95% confidence level with the $\xi_2$ equal to 19.269 before and 5.257 after tilt correction; the critical value is 5.583 at this confidence level. Further analysis using the Watson and Enkin's (1993) test presents an optimal concentration at 105.9% unfolding with 95% uncertainty ranging from 99.4 to 112.7% unfolding (Fig. 4c) and is strongly indicative of a pre-folding origin for the ChRM. Therefore, the ChRM has both positive fold and reversal test results strongly supporting the interpretation that the stable ChRMs resolved either by AF treatment between 20 and 89 mT (Zongpu Formation) or by thermal demagnetization between 500–

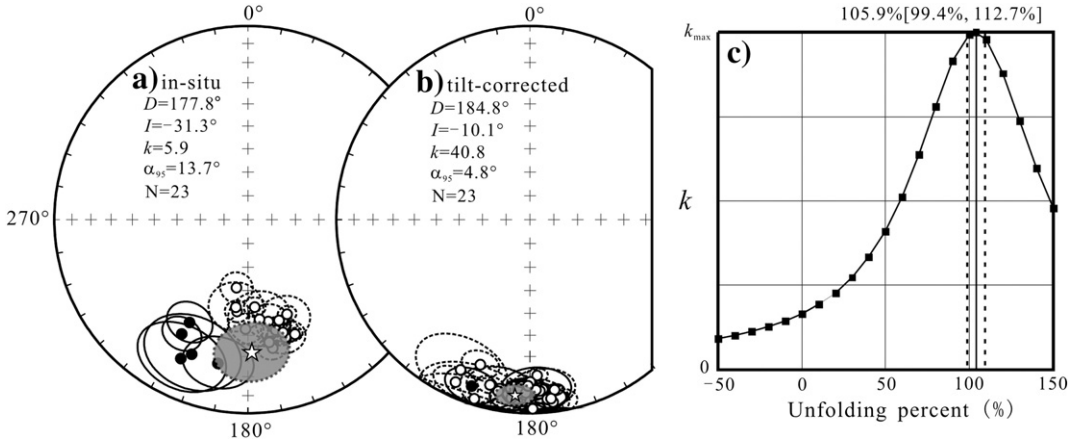


**Fig. 4.** (a, b) Equal-area projections of site-mean directions of the ChRM before and after tilt adjustment for Member I of the Zongpu Formation from both the A and C sections. (c) Incremental unfolding analysis (Watson and Enkin, 1993) for the ChRM isolated from Member I of the Zongpu Formation indicative of a pre-folding origin. Symbols are as for Fig. 3.

590 °C and 610–670 °C (Jidula Formation) are primary components acquired at, or near to, the time of rock formation.

## 5. Magnetostratigraphy

Directions of ChRM from 167 horizons of sections A and B were used to calculate virtual geomagnetic pole (VGP) latitudes and the sections were organized into stratigraphic levels referred to the declination and the VGP latitude (Fig. 5) to define magnetic polarity zones. The two studied sections are separated by about 2 km (Fig. 1b) and were correlated in the field using a sharp lithological change from limestone to sandstone.

As shown in Fig. 5, the reconstructed magnetic polarity sequence is dominated by reversed polarity and is very similar to the geomagnetic polarity time scale (GPTS, Ogg and Smith, 2004) in the Paleocene, confirming the biostratigraphic age provided by the paleontological evidence (Wan et al., 2002a, b; Willems and Zhang, 1993). Only two short normal polarities can be identified. Although we are unable to correlate the magnetic polarity sequence to the GPTS independently, detailed biostratigraphic studies make it possible to build a magnetostratigraphy. As elaborated before, the end of the Thanetian (55.8–58.7 Ma) occurs at the boundary of Member III and Member IV of the Zongpu Formation (Willems and Zhang, 1993). It is then reasonable to correlate the first normal polarity zone (N1) at the upper part of the Member III to chron C25n (56.67–57.18 Ma). Meanwhile, noting that the bottom of the Zongpu Formation has a Danian age (Willems and Zhang, 1993) and that the magnetic polarity sequence is still dominated by reversed polarity (R3) in upper Jidula Formation, the second normal polarity zone (N2) near the boundary of the Zongpu and Jidula formations appears to correlate to chron C27n (61.65–61.938 Ma) instead of chron C26n or C28n. Unfortunately, chron C26n was not identified in the magnetic polarity sequence, perhaps due to a sampling interval which was too large in some segments, or to the poor paleomagnetic record in some of the marl horizons.

Therefore, a combined age determination provided by both biostratigraphy and magnetostratigraphy provides age control points for the sampled succession (Fig. 5). Given that marine sedimentation in the Zongpu Formation was evidently subject to a relatively stable rate of deposition, we infer a deposition rate of ~6.3 cm/ka between the two magnetostratigraphic ages at 33.8 m (56.7 Ma) and 350.4 m (61.7 Ma). Noting that the boundary between Member I and II of the Zongpu Formation is constrained to be near the bottom of the Thanetian (~58.7 Ma) by biostratigraphy (Willems and Zhang, 1993), we identify a very similar magnetostratigraphic age (~58.8 Ma) by linear interpolation of the deposition rate. This confirms that the assumption of a quasi-uniform deposition rate for the Zongpu Formation is correct to a first-order and allows us to compute magnetostratigraphic ages for the other boundaries of the sub-units of the Zongpu Formation; thus the top and base of the sampled Zongpu Formation are estimated to have ages of ~56.2 and ~61.8 Ma, respectively (Fig. 5).

However, because of the limited number of available specimens in Members II, III, and VI of the Zongpu Formation, we have reorganized the sampled part of the Zongpu Formation into two statistical divisions: (i) the upper part of the Zongpu Formation (Member II, Member III and Member VI, 0–163.7 m), and (ii) the lower part of the Zongpu Formation (Member I, 166.4–356.4 m); the corresponding magnetostratigraphic ages of these two units are ~56.2–58.8 Ma and ~58.8–61.8 Ma, respectively. The calculated unit-mean directions and corresponding paleomagnetic poles are listed in Table 1.

## 6. Discussions

To examine the influence of inclination shallowing which is generally present in sedimentary rocks, an Elongation/Inclination (E/I) analysis (Tauxe, 2005) has been performed on 167 independent ChRMs used to construct the magnetic polarity sequence for the Zongpu and upper Jidula formations. Since only one available ChRM direction was resolved from each sedimentary horizon, the procedure satisfies the requirement that each direction is an independent sample of the geomagnetic field (Tauxe, 2005). As shown in Fig. S2, the E/I analysis yielded a mean inclination of 17.9° with 95% confidence ranging from 13.9° to 22.3°. The original inclination (12.6°) falls outside of this confidence interval and seems to be slightly influenced by compaction-induced shallowing. This is compatible with the E/I analysis result of a published Paleogene data set in the Tethyan Himalaya reported by Dupont-Nivet et al. (2010). The application of an E/I correction in this latter study yielded only small inclination corrections (~5°) resulting in a paleolatitudinal position similar to the original result before correction (Dupont-Nivet et al., 2010), thus confirming that compaction-induced inclination shallowing in the Tethyan Himalayan sediments is insignificant or very slight. The significance of possible slight shallowing will be discussed later (Section 6.2).

### 6.1. Position of the northern margin of the Indian plate

New paleomagnetic poles for the upper and lower parts of the Zongpu Formation were calculated from the ChRM directions before E/I correction (Table 1 and S1) and indicate that the Tethyan Himalaya (reference site: 29.3°N, 88.5°E) was located at paleolatitudes ranging from 6.6°N ± 3.5° (~59–62 Ma) to 11.1°N ± 2.5° (~56–59 Ma) during

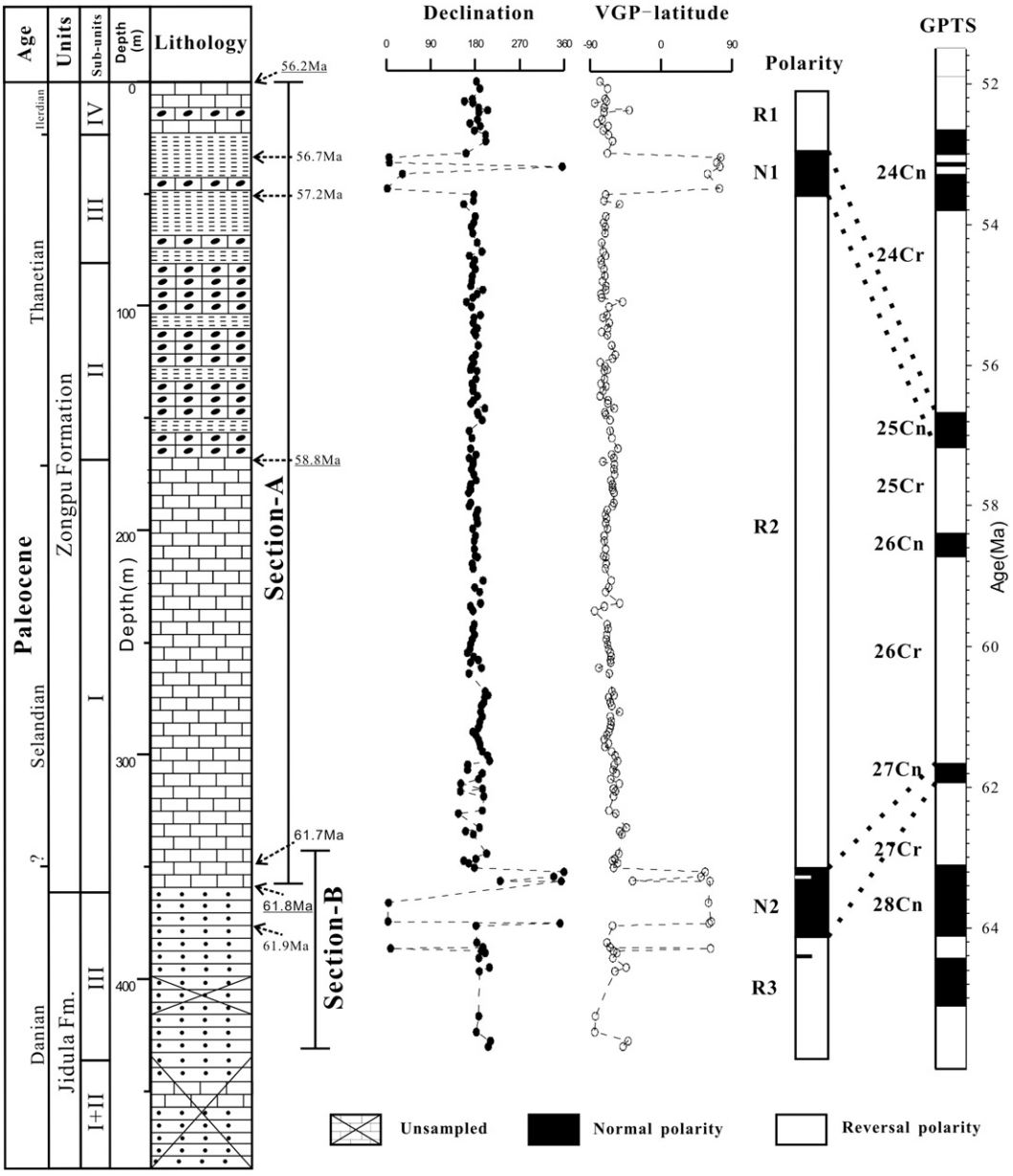


**Fig. 5.** Lithologic and magnetostratigraphic results from sections A and B in the Gamba area of southern Tibet with declinations and VGP latitudes plotted as a function of stratigraphic level and showing the correlation with the GPTS (Ogg and Smith, 2004). Magnetochrons defined by only one horizon are shown by short-half bars. Lithologic legends are as for Fig. 1. A combined age of magnetostratigraphy with deposition rate linearly interpolated (underlined) is marked at critical boundaries with an arrow on the right side of rock stratigraphic succession.

Paleocene times. The former result is compatible with that estimated from an earlier paleomagnetic study on the Zongpu Formation in the Gamba and Duela areas (Patzelt et al., 1996) and confirms that the Tethyan Himalaya was located at lower latitudes in the Northern Hemisphere during deposition of the Zongpu Formation. However, the results are noticeably different from those estimated from the Zongpu Formation in the Dingri area, in which the Tethyan Himalaya was suggested to have a much more southerly position of 3.0°S ± 5.3° (Besse et al., 1984) and 15.7°S ± 4.0° (Tong et al., 2008) during deposition of the Zongpu Formation. This discrepancy could result from a sedimentation age difference of the Zongpu Formation between the Dingri and Gamba areas and/or serious remagnetization in the Dingri area resulting in only a few sampling sites preserving primary remanence (Besse et al., 1984; Tong et al., 2008). Alternatively, a paleolatitudinal difference between the Dingri and Gamba areas during deposition of the Zongpu Formation could indicate a vast collision-related deformation of the northern margin of Greater India. As suggested by Ding et al. (2005), the central part of the Tethyan Himalaya may have the shape of a northward-protruded triangle implying that the Gamba area was located north of the Dingri area during deposition of the Zongpu Formation.

On the other hand, Patzelt et al. (1996) also reported a late Cretaceous paleopole from the Zongshan marine sediments in the Gamba area. This is the only reliable late Cretaceous paleopole from the Tethyan Himalaya and indicates a lower paleolatitude of ~4.7°S ± 4.4° for the northern margin of the Indian plate during deposition of the Zongshan Formation (Figs. 6–7 and Table S1). Comparison between this late Cretaceous paleopole and the newly-obtained result from the lower part of the Zongpu Formation (Fig. 7) indicates a considerable poleward transport of 11.3° ± 4.5° and confirms that the Himalayan terrane was in rapid northward motion during deposition of the Zongshan and Jidula formations (Fig. 8a–b). Moreover, a poleward transport of 4.5° ± 3.4° detected from the lower and upper Zongpu formations (Fig. 7) further suggests that the northward displacement was continuing during deposition of the Zongpu Formation (Fig. 8b–c).

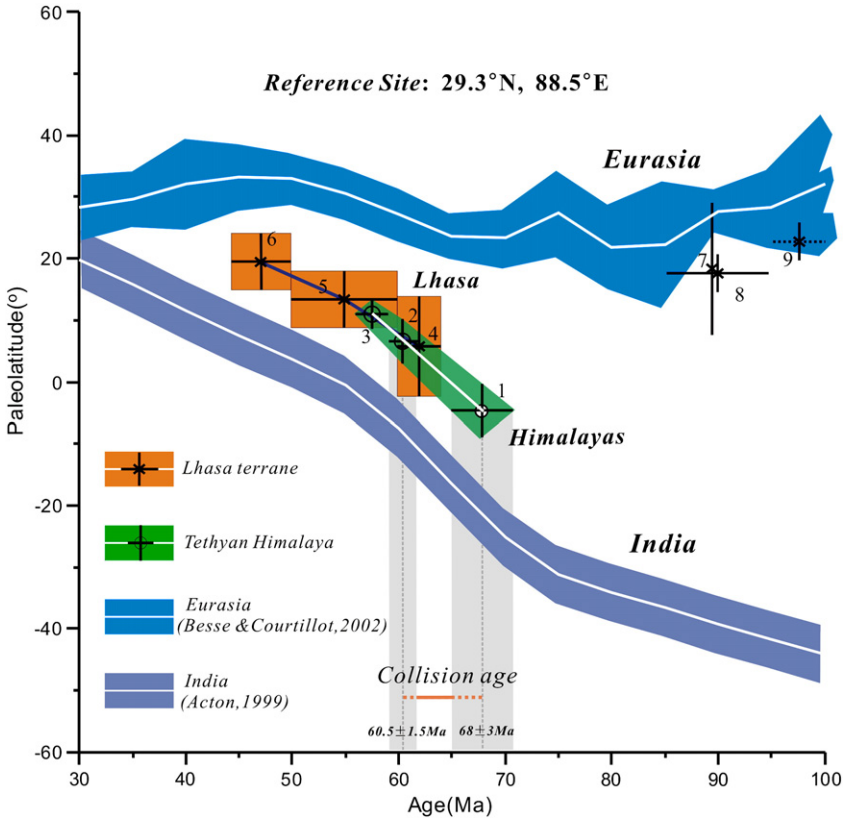


**Fig. 6.** Paleolatitudinal comparison within India, Eurasia, Himalayas, and Lhasa during post-late Cretaceous times. The numbers 1, 2, and 3 indicate average paleolatitudes for the Himalayas estimated from paleomagnetic results isolated from the Zongshan (Patzelt et al., 1996), lower Zongpu and upper Zongpu (this study) formations; the numbers 4, 5, 6 represent average paleolatitudes for the Lhasa terrane during formation of the Dianzhong, Nianbo and Pana formations (Chen et al., 2010; Dupont-Nivet et al., 2010; Liebke et al., 2010; Sun et al., 2010), whilst the numbers 7, 8, 9 show mean paleolatitudes for the Lhasa terrane in middle to late Cretaceous (Lin and Watts, 1988; Tan et al., 2010) times, respectively. See Table S1 for details. The discrepancy in paleolatitudes for the Lhasa terrane between the late Cretaceous and early Paleogene very likely resulted from a slight southward motion of Eurasia during this time interval.

### 6.2. Timing of the initial contact between India and Asia

Late Cretaceous to Paleogene paleomagnetic data obtained from both sides of the IYSZ comprising the Tethyan Himalaya, Lhasa and Qiangtang terranes are summarized in Table S1. The paleoposition of the southern margin of Eurasia has been recently well-constrained by several paleomagnetic studies on the Linzizong Group developed in the Lhasa terrane (Chen et al., 2010; Dupont-Nivet et al., 2010; Liebke et al., 2010; Sun et al., 2010; Tan et al., 2010). These studies have yielded a consensus for the paleomagnetic record in the Dianzhong and Nianbo formations. However, controversy still exists about the record in the Pana Formation where most studies identify latitudes less than 22°N (Chen et al., 2010, in progress; Dupont-Nivet et al., 2010); in contrast Tan et al. (2010) reported a paleolatitude as high as 33.0° ± 5.7°N. Liebke et al. (2010) argued that this result might have biased by an insufficient sampling of the geomagnetic field. Our recent investigation on lava flows in a quarry of the Pana Formation in the Linzhou Basin (sampling section of Tan et al., 2010) indicates both normal and reversed characteristic remanence directions with distinctively different moderate to steep inclinations coexisting even in one sampling site (our unpublished data). On the other hand, a more recent study of late Paleogene volcanics from the Qiangtang terrane indicates that the southern margin of the Lhasa terrane was located as far south as 20°N throughout Eocene times (Lippert et al., 2011). Hence we prefer to use newly published compatible paleopoles to calculate formation-mean poles for the Linzizong Group in the Lhasa terrane; these are located at 66.0°N, 284.9°E ($A_{95}$ = 8.5°), 73.6°N, 269.5°E ($A_{95}$ = 4.6°), and 76.5°N, 224.1°E ($A_{95}$ = 4.7°) for the Dianzhong (64–60 Ma), Nianbo (60–50 Ma), and Pana (50–44 Ma) formations, respectively. Accordingly, we predict that the Lhasa terrane was located at 6.1°N ± 8.5°, 12.9°N ± 4.6°, and 19.3°N ± 4.7° during formation of the Dianzhong, Nianbo, and Pana formations, respectively.

As shown in Fig. 7, our new Paleocene paleopoles for the Tethyan Himalaya during 59–62 Ma and 56–59 Ma identify no discernible poleward transport of 0.5° ± 7.3° and 1.8° ± 4.2° between these two paleopoles and coeval poles from the Lhasa terrane during formation of the Dianzhong (~64–60 Ma) and Nianbo (~60–50 Ma) formations, respectively. This indicates that the initial contact between India and Asia should have occurred no later than 60.5 ± 1.5 Ma. Critical to this case we note that the paleopole for late Cretaceous marine sediments (Zongshan Formation, 65–71 Ma) in the Gamba area (Tethyan Himalaya, Patzelt et al., 1996) yielded a paleolatitude as far south as 4.7°S ± 4.4° just inside the Southern Hemisphere, and that the southern margin of the Asian continent (i.e. the Lhasa terrane) was located at low latitudes in the Northern Hemisphere throughout late Cretaceous and Paleocene times. This means that a paleolatitudinal gap of 10.8° ± 7.7° is predicted to have existed between the Indian and Asian continents at 68 ± 3 Ma. Thus the initial contact between India and Asia should have occurred no earlier than 68 ± 3 Ma. Therefore, the probable age for the onset of the collision lies between 60.5 ± 1.5 and 68 ± 3 Ma (Fig. 7). Moreover, the minor contributions of limited shortening between the sampling location and the IYSZ (<130–140 km, Ratschbacher et al., 1994), crustal shortening in northern India before 60.5 ± 1.5 Ma (~400 km, Section 6.1), and the possibility of slight inclination shallowing (~200–300 km) would permit a

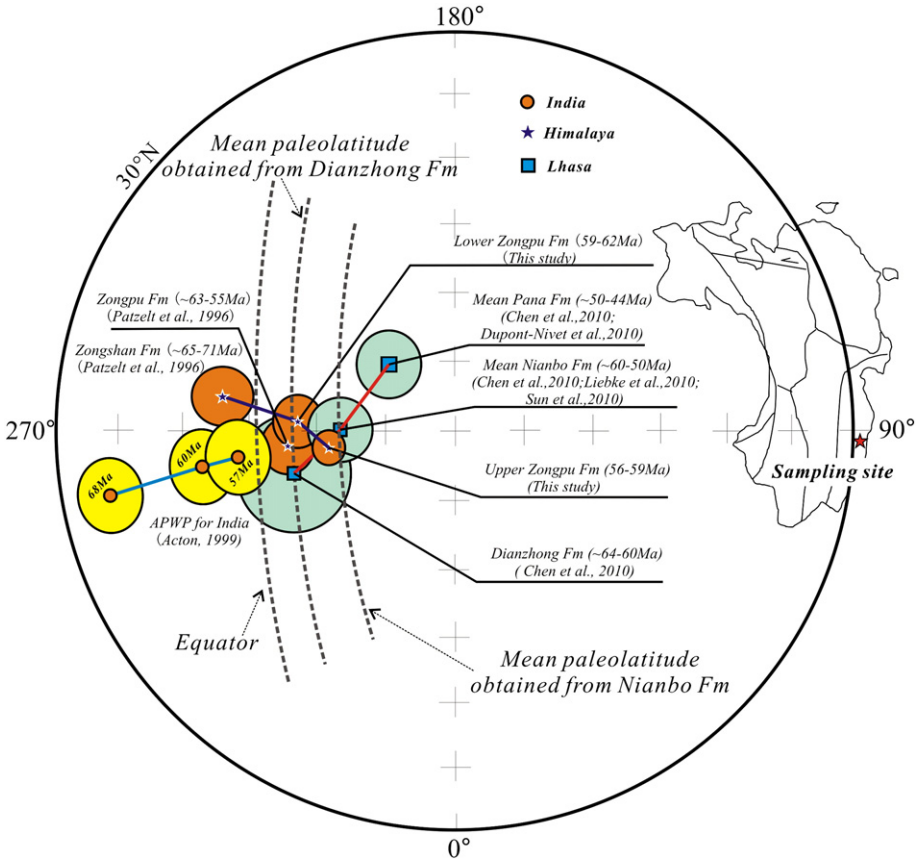


**Fig. 7.** Equal-area projection showing paleomagnetic comparisons within late Cretaceous to Paleogene paleopoles from the Tethyan Himalaya (Patzelt et al., 1996 and this study), Lhasa terrane (Chen et al., 2010; Dupont-Nivet et al., 2010; Liebke et al., 2010; Sun et al., 2010), and the Indian plate (Acton, 1999). All the data are plotted in the Northern Hemisphere.

collision age slightly earlier than 60.5 ± 1.5 Ma. The total contribution of shortening could be as large as ~700–800 km and noting that the motion rate of India is ~200 km/Ma during these times (Acton, 1999), the most probable collision age is estimated to be ~65 Ma. Thus we argue that onset of the India–Asia collision is very likely to have occurred near the *K*/*Pg* boundary, which is compatible with substantial geophysical, geological, geochemical and paleontological evidence (e.g. Beck et al., 1995; Briggs, 2003; Chen et al., 2010; Jaeger et al., 1989; Klootwijk et al., 1992; Rage, 2003 and references therein). In particular, the regionally-distinct unconformity between the Dianzhong volcanic rocks (lowest unit of the Linzizong Group) and underlying upper Cretaceous red sediments in the Lhasa terrane has been repeatedly argued to have formed in response to the India–Asia collision (e.g., Ding et al. (2005, 2007); Huang et al., 2005b; Mo et al., 2003, 2008; Pan and Ding, 2005) consider that simultaneous, large-scale deformation occurred on both sides of the IYSZ around the *K*/*Pg* boundary indicating that the India and Asian continents should have collided by then, at least in the central part of the suture zone. More recently, lithic sandstones of the Sandanlin and Zheya formations with an age of 65–56 Ma developed in the middle part of the suture zone near the city of Saga (Ding, 2003) have been proved to have a provenance in the Gandese magmatic arc (Wang et al., 2011). In addition a detailed petrographic study, in-situ detrital zircon U–Pb ages and Lu–Hf isotopic analyses, whole rock Nd-isotopes, and Cr-spinel electronic microprobe data from late Cretaceous clastic sedimentary rocks of the Tethys Himalaya near the city of Gyangze, southern Tibet, have suggested a rapid change of provenance from southern India to the northern arc (Cai et al., 2011). These studies clearly show an input of Asian detrital material to the passive margin of India near the collision age predicted by this study.

### 6.3. Crustal shortening in the Himalayas and the size of Greater India

Together with the late Cretaceous paleopole obtained from the Zongshan Formation in the Gamba area (Patzelt et al., 1996), the size of Greater India just before the collision as well as the post-collisional crustal shortening within the Himalayas can be estimated from a comparison between late Cretaceous and Paleocene paleopoles for the Tethyan Himalaya and the apparent polar wander path (APWP) of the Indian plate, which has been well-constructed by Acton (1999). Similar to the suggestions raised by Patzelt et al. (1996), latitudinal shortening within the Himalayas has been constrained between 1500 ± 480 km and 1900 ± 570 km (Table 2). This implies that the Greater Indian plate may have had a northern extension of at least 1500 ± 480 km beyond its present northern margin, at least in the central part of the suture zone. Moreover, most of the crustal shortening (1500 ± 480 km) is further constrained to have taken place after deposition of the Zongpu Formation (57.5 ± 1.5 Ma), although an earlier shortening of ~400 km may have occurred during the interval between 68 ± 3 Ma and 57.5 ± 1.5 Ma (Fig. 8a–c and Table 2).

There is a consensus that large-scale post-collisional crustal shortening and thickening should have occurred within the Himalayas by folding and thrusting (e.g., Decelles et al., 2002; Yin and Harrison, 2000), and most researchers believe that it is likely to have been at least several hundreds of kilometers (e.g. Decelles et al., 2002; Johnson, 2002; Yin et al., 2006, 2010). However, models for Greater India are controversial and its northern extension has been considered to range from a few hundreds to more than one thousand kilometers beyond the present margin of India (see Ali and Aitchison, 2005 for a detailed review). In particular, Ali and Aitchison (2005) propose a model of Greater India based on a Gondwanan reconstruction immediately prior

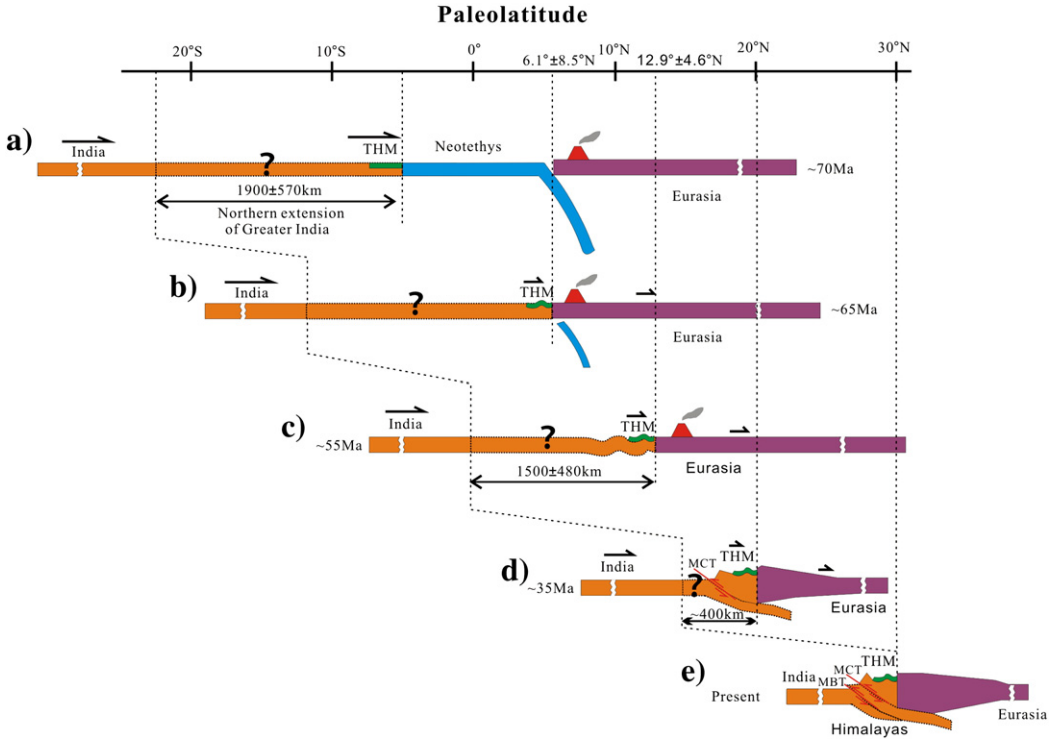


**Fig. 8.** Conceptional model describing geodynamic evolution of the India–Asia collision in post-late Cretaceous times (approximately a S–N profile). The northern margin of India is defined as the Indus–Yarlung Zangbo suture zone. See text for details.

to rifting and break-up of the western and eastern segments of the Gondwana at ~160 Ma, in which Greater India was constrained to have had a northern extension of ~950 km beyond its present north-central margin at the Wallaby–Zenith fracture zone. However, the Exmouth Plateau, located ~600 km northeast of the Wallaby–Zenith fracture, provides an equally reliable alternative for the northern margin of Greater India prior to the rifting and break-up (e.g. Larson, 1977; Sahabi, 1993); in this case the northern extent of Greater India could be as large as ~1500 km, which is in good agreement with paleomagnetic results from late Cretaceous to Paleocene marine sediments in the Tethyan Himalaya (Patzelt et al., 1996 and this study).

The large northern extension of Greater India (1500 ± 480 km or more) seems to conflict with balanced cross-section analyses from various parts of the Himalayas, which suggest an amount of 670–775 km of shortening within the Himalayas (DeCelles et al., 2002; Yin et al., 2010). However, balanced cross-section analyses can result in considerable errors at big discontinuities (due to subduction or hidden subduction zones) if large amounts of subduction have occurred at for example, on the MCT; for this reason it is possible for this approach to underestimate tectonic shortening within the Himalayas (Johnson, 2002). We consider that the deficit of ~700–800 km or more between the observed crustal shortening within the Himalayas and our estimate may have been accommodated by subduction of the Indian lithosphere below the Himalayas and Eurasia. Indeed, geophysical investigations have shown that Greater India may have subducted below the Asian continent far north of the IYSZ (Kind et al., 2002; Owens and Zandt, 1997; Zhang and Klemperer, 2010; Zhao et al., 1993, 2001).

### 6.4. Initial activation of the MCT

The newly obtained Paleocene paleopole for the Tethyan Himalaya (59–62 Ma) is not significantly different from that for the Lhasa terrane (~64–60 Ma) (Fig. 7), suggesting that no paleomagnetically-detectable crustal shortening has occurred on the IYZS since at least 60.5 ± 1.5 Ma (Fig. 8b–e). However, direct comparison between stable India and the Lhasa terrane suggests that a crustal shortening of 1500 ± 580 km should have happened after ~55 Ma (Table 2); therefore, this large scale post-collisional shortening should have been accommodated in the Himalayas instead of on the IYSZ. Furthermore, this shortening cannot be explained by the "observable" folding and thrusting in the Himalayas without large scale subduction of India below Asia (see Section 6.3); the big discontinuities (e.g. MCT) are thus required to accommodate the "excess" crustal shortening (Fig. 8c–e). In fact, geologic studies have shown that the subduction zone between India and Asia had migrated southward since the initial collision (e.g. Gansser, 1991; Le Fort, 1975).

On the other hand, recent paleomagnetic investigations of the Linzizong Group yield lower paleolatitudes ranging from 6.1°N ± 8.5° to 19.3°N ± 4.7° for the Lhasa terrane during the interval ~64–44 Ma (See Section 6.2). This view has been further corroborated by

**Table 2**
Crustal shortening among the Tethyan Himalaya, Indian Plate and Lhasa terrane during the India–Asia collision.

| Age (Ma) | Terrane | Observed pole | | | | Reference pole (Acton, 1999) | | | Rotation (°) | Latitudinal shortening (km) |
|---|---|---|---|---|---|---|---|---|---|---|
| | | Latitude (°) | Longitude (°) | A95 (°) | Reference | Latitude (°) | Longitude (°) | A95 (°) | | |
| 56–59 | Himalaya | 71.6 | 277.8 | 2.5 | This study | 58.3 | 276.7 | 4.7 | 1.3 ± 4.3 | 1500 ± 480 |
| 59–62 | Himalaya | 67.3 | 266.3 | 3.5 | This study | 52.8 | 277.9 | 4.7 | 6.6 ± 4.7 | 1600 ± 520 |
| 65–71 | Himalaya | 55.8 | 261.4 | 4.4 | Patzelt et al., 1996 | 38.1 | 280.7 | 4.7 | 3.0 ± 5.4 | 1900 ± 570 |
| 60–50 | Lhasa | 73.6 | 269.5 | 4.6 | See Table S1 | 59.9 | 276.3 | 4.7 | 3.6 ± 5.3 | 1500 ± 580 |

paleomagnetic study of ~30–40 Ma volcanic rocks from central Tibet (Lippert et al., 2011); this suggests that the Lhasa terrane was sited as far south as 20°N throughout Eocene times. However, in the light of the APWP of India (Acton, 1999), the current northern margin of India may have been at 16°N ± 4.7° during the latest Eocene (~35 Ma). This indicates that ~1100 km or more of tectonic shortening should have been absorbed by this time taking into account the 1500 ± 480 km northern extension of Greater India. Such a large scale crustal shortening can hardly have been absorbed by the Himalayas without subduction of India below Asia (see Section 6.3); thus the initiation of large scale subduction of India below Asia as well as activation of the MCT is very likely to have occurred as early as ~35 Ma (Fig. 8d). This view is compatible with new Zircon SHRIMP U–Pb dating of the Yalaxaingbo granite in the Tethyan Himalaya which indicates that the emplacement of the Yalaxaingbo pluton, as well as activation of the MCT, occurred as early as ~45–35 Ma (Qi et al., 2008; Xu et al., 2011; Zeng et al., 2009).

## 7. Conclusions

In the light of paleontological constraints on the Zongpu marine sediments in the Tethyan Himalaya, magnetostratigraphic investigations date the Zongpu Formation in the Gamba area at ~56.2–61.8 Ma. Further paleomagnetic analysis has yielded two paleomagnetic poles, at 71.6°N, 277.8°E with $A_{95} = 2.5°$ and 67.3°N, 266.3°E with $A_{95} = 3.5°$ for the upper (~56–59 Ma) and lower (~59–62 Ma) parts of this formation respectively. The available paleomagnetic constraints on the kinematics of the terranes at both sides of the IYSZ, as well as a conceptional model for the India–Asia collision in its the early stages, are summarized in Fig. 8:

(1) The Tethyan Himalayan terrane, i.e. the northern margin of Greater India, may still have been located as far south as 4.7°S ± 4.4° just south of the equator during late Cretaceous times and continued its fast northward transport during deposition of the Zongshan Formation. The Lhasa terrane was located at low latitudes in the Northern Hemisphere during these times (Fig. 8a).
(2) Paleopoles from the lower Zongpu Formation (Member I, ~62–59 Ma) in the Tethyan Himalaya and the Dianzhong volcanics (~64–60 Ma) in the Lhasa terrane essentially overlap predicting no significant poleward transport of 0.5° ± 7.3° between them and suggesting that an initial contact between the Tethyan Himalaya and Lhasa terranes should have been established prior to 60.5 ± 1.5 Ma (Fig. 8b). We argue that onset of the India–Asia collision most likely occurred near the *K*/*P*g boundary, at least in the central part of the IYSZ. This is in agreement with a large body of geological and geochemical evidence.
(3) The poleward transport of 4.5° ± 3.4° for the Himalayan terrane during deposition of the Zongpu Formation (~62–56 Ma) suggests that the Tethyan Himalaya continued its northward movement during this interval. Comparison between Paleocene paleopoles from the Zongpu Formation in the Tethyan Himalaya and coeval ones for the Indian plate (Acton, 1999) suggests a northern extension of Greater India of at least 1500 ± 480 km prior to onset of the India–Asia collision. The majority of this crustal shortening may have been absorbed by folding and thrusting within the Himalayas and subduction of India below Asia after 57.5 ± 1.5 Ma) (Fig. 8c–d).
(4) The Lhasa terrane was probably still located as far south as 20°N throughout Eocene times (Lippert et al., 2011), however, the current leading edge of continental India may have arrived at 16°N ± 4.7° by ~35 Ma, implying that considerable crustal shortening (~1100 km or more) should have occurred within the Himalayas as early as ~35 Ma and resulted in large scale subduction of India below Asia as well as activating the MCT (Fig. 8d).

Nonetheless, all the conclusions above are based upon paleomagnetic studies carried out within limited areas in the central part of the Tethyan Himalaya and Lhasa terranes. For a suture zone extending ~2500 km in approximately an east–west direction, much more paleomagnetic study is desirable to better understand the full history of the India–Asia collision. In addition our interpretation of the northern extension of Greater India and the timing of onset of the India–Asia collision is undoubtedly based on the assumption that the Tethyan Himalaya is a part of the passive margin of Greater India. Although this is favored by most researchers recent studies carried out by Liu et al. (Li et al., 2010; Liu et al., 2010) suggest that the Tethyan Himalaya could be a part of the Lhasa terrane or an interoceanic arc within the Neo-Theyan Ocean. Hence more detailed investigations of the APW path of the Tethyan Himalaya during Cretaceous to Paleogene times is required to determine paleopositions for the Tethyan Himalaya relative to India and the Lhasa terrane and could play an important part in accurately understanding the onset of the India–Asia collision.

## Acknowledgments

We thank Zhonghai Zhuang and Bu Qiong for field assistance and acknowledge Drs. Wenjiao Xiao and John D.A. Piper for helpful discussions and comments. We also appreciate Mark Harrison (Editor), Guillaume Dupont-Nivet and two anonymous reviewers for insightful comments and suggestions. This work was supported by the Key Items of Knowledge Innovation Programs of the Chinese Academy of Sciences (KZCX2-YW-Q09-01) and the National Natural Science Foundation of China (41072156).

## Appendix A. Supplementary data

Supplementary data to this article can be found online at doi:10.1016/j.epsl.2011.07.001.

## References

Acton, G.D., 1999. Apparent polar wander of India since the Cretaceous with implications for regional tectonics and true polar wander. In: Radhakrishna, T., et al. (Ed.), The Indian Subcontinent and Gondwana: A Palaeomagnetic and Rock Magnetic Perspective: Geol. Soc. India Mem., 44, pp. 129–175.
Aitchison, J.C., Ali, J.R., Davis, A.M., 2007. When and where did India and Asia collide? J. Geophys. Res. 112 (B05423), 1–12.
Aitchison, J.C., Zhu, B.D., Davis, A.M., Liu, J.B., Luo, H., Malpas, J.G., McDermid, I.R.C., Wu, H.Y., Ziabrev, S.V., Zhou, M.F., 2000. Remnants of a Cretaceous intra-oceanic subduction system within the Yarlung–Zangbo suture (southern Tibet). Earth Planet. Sci. Lett. 183, 231–244.
Aitchison, J.C., Davis, A.M., 2001. When did the India–Asia collision really happen? Gondwana Res. 4, 560–561.
Ali, J.R., Aitchison, J.C., 2005. Greater India. Earth Sci. Rev. 72, 169–188.
Ali, J.R., Aitchison, J.C., 2008. Gondwana to Asia: Plate tectonics, paleogeography and the biological connectivity of the Indian sub-continent from the Middle Jurassic through latest Eocene (166–35 Ma). Earth Sci. Rev. 88, 145–166.
Allègre, C.J., Courtillot, V., Tapponnier, P., et al., 1984. Structure and evolution of the Himalaya–Tibet orogenic belt. Nature 307, 17–22.
Appel, E., Muller, R., Widder, R.W., 1991. Paleomagnetic results from the Tibetan sedimentary series of the Manang area (North central Nepal). Geophys. J. Int. 104, 255–266.
Appel, E., Patzelt, A., Chouker, C., 1995. Secondary palaeoremanence of Tethyan sediments from the Zanskar Range (NW Himalaya). Geophys. J. Int. 122, 227–242.
Beck, R.A., Burbank, D.W., Sercombe, W.J., et al., 1995. Stratigraphic evidence for an early collision between northwest India and Asia. Nature 373, 55–58.
Besse, J., Courtillot, V., Pozzi, J.P., Westphal, M., Zhou, Y.X., 1984. Paleomagnetic estimates of crustal shortening in the Himalayan thrusts and Zangbo suture. Nature 311, 621–626.
Briggs, J.C., 2003. The biogeographic and tectonic history of India. J. Biogeogr. 30, 381–388.
Brookfield, M.E., 1998. The evolution of the great river systems of southern Asia during the Cenozoic India–Asia collision: rivers draining southwards. Geomorphology 22, 285–312.
Cai, F.L., Ding, L., Yue, Y.H., 2011. Provenance analysis of upper Cretaceous strata in the Tethys Himalaya, southern Tibet: implications for timing of India–Asia collision. Earth Planet. Sci. Lett. 305 (1–2), 195–206.
Chang, C.F., Chen, N.S., Coward, M.P., et al., 1986. Preliminary conclusions of the Royal-Society and Academia-Sinica 1985 geotraverse of Tibet. Nature 323, 501–507.

Chen, J.S., Huang, B.C., Sun, L.S., 2010. New constraints to the onset of the India–Asia collision: paleomagnetic reconnaissance on the Linzizong Group in the Lhasa Block, China. Tectonophysics 489, 189–209.
Clark, M.K., Schoenbohm, L.M., Royden, L.H., Whipple, K.X., Burchfiel, B.C., Zhang, X., Tang, W., Wang, E., Chen, L., 2004. Surface uplift, tectonics, and erosion of eastern Tibet from large-scale drainage patterns. Tectonics 23 2002TC001402.
DeCelles, P.G., Robinson, D.M., Zant, G., 2002. Implications of shortening in the Himalayan fold-thrust belt for uplift of the Tibetan Plateau. Tectonics 21 (6).
Dewey, J.F., Cande, S., Pitman, W.C., 1989. Tectonic evolution of the India Eurasia Collision Zone. Eclogae Geol. Helv. 82, 717–734.
Ding, L., 2003. Paleocene deep-water sediments and radiolarian fauna: implications for evolution of Yarlung Zangbo foreland basin, southern Tibet. Sci. China D 33, 47–58 (in Chinese).
Ding, L., Kapp, P., Wan, X.Q., 2005. Paleocene–Eocene record of ophiolite obduction and initial India–Asia collision, south central Tibet. Tectonics 24 (TC3001), 1–18.
Ding, L., Kapp, P., Yue, Y., Lai, Q., 2007. Postcollisional calc-alkaline lavas and xenoliths from 987 the southern Qiangtang terrane, central Tibet. Earth Planet. Sci. Lett. 254, 28–38.
Ding, L., Kapp, P., Zhong, D.L., Deng, W.M., 2003. Cenozoic volcanism in Tibet: evidence for a transition from oceanic to continental subduction. J. Petrol. 44, 1833–1865.
Dupont-Nivet, G., Lippert, P.C., van Hinsbergen, D.J.J., Meijers, M.J.M., Kapp, P., 2010. Palaeolatitude and age of the Indo-Asia collision: palaeomagnetic constraints. Geophys. J. Int. 182, 1189–1198.
Fisher, R.A., 1953. Dispersion on a sphere. Proc. R. Soc. Lond. A 217, 295–305.
Gansser, A., 1964. The Geology of the Himalayas. Wiley, New York, NY. 289 pp.
Gansser, A., 1991. Facts and theories on the Himalayas. Eclogae Geol. Helv. 84, 33–59.
Hedberg, H.D., 1970. Continental margins from viewpoint of the petroleum geologist. AAPG Bull. 54.
Huang, B.C., Chen, J.S., Yi, Z.Y., 2010. Paleomagnetic discussion of when and where India and Asia initially collided. Chin. J. Geophys. 53 (9), 2045–2058.
Huang, Y.C., Yang, D.M., Zheng, C.Q., He, Z.H., Dai, L.N., Li, J.G., Zhang, Y.Y., 2005b. The geochemical characteristics of the Pana volcanic rocks of the Linzizong Group in the Zhaxue area, Linzhou County, Tibet and its geological implication. J. Jilin Univ. (Earth Sci. edition) 35 (5), 576–580 (in Chinese).
Jaeger, J.J., Courtillot, V., Tapponnier, P., 1989. Paleontological view of the ages of the Deccan Traps, the Cretaceous Tertiary/boundary, and the India–Asia collision. Geology 17, 316–319.
Johnson, M.R.W., 2002. Shortening budgets and the role of continental subduction during the India–Asia collision. Earth Sci. Rev. 59, 101–123.
Kind, R., Yuan, X., Saul, J., Nelson, D., Sobolev, S.V., Mechie, J., Zhao, W., Kosarev, G., Ni, J., Achauer, U., Jiang, M., 2002. Seismic images of crust and upper mantle beneath Tibet: evidence for Eurasian plate subduction. Science 298, 1219–1221.
Kirschvink, J.L., 1980. The least-square line and plane and the analysis of paleomagnetic data. Geophys. J. R. Astron. Soc. 62, 699–718.
Klootwijk, C.T., Gee, J.S., Peirce, J.W., Smith, G.M., Mcfadden, P.L., 1992. An early India–Asia contact-paleomagnetic constraints from Ninetyeast Ridge, ODP Leg 121. Geology 20, 395–398.
Larson, R., 1977. Early Cretaceous break up of Gondwanaland of western Australia. Geology 5, 57–60.
Le Fort, P., 1975. Himalayas: the collided range. Present knowledge of the continental arc. Am. J. Sci. 275A, 1–44.
Li, G.W., Liu, X.H., Pullen, A., Wei, L.J., Liu, X.B., Huang, F.X., Zhou, X.J., 2010. In-situ detrital zircon geochronology and Hf isotopic analyses from Upper Triassic Tethys sequence strata. Earth Planet. Sci. Lett. 297, 461–470.
Liebke, U., Appel, E., Ding, L., Neumann, U., Antolin, B., Xu, Q., 2010. Position of the Lhasa terrane prior to India–Asia collision derived from palaeomagnetic inclinations of 53 Ma old dykes of the Linzhou Basin: constraints on the age of collision and post-collisional shortening within the Tibetan Plateau. Geophys. J. Int. 182, 1199–1215.
Lin, J., Watts, D.R., 1988. Palaeomagnetic results from the Tibetan Plateau. Phil. Trans. R. Soc. A 327, 239–262.
Lippert, P.C., Zhao, X.X., Coe, R.S., Lo, C.H., 2011. Palaeomagnetism and $^{40}Ar/^{39}Ar$ geochronology of upper Palaeogene volcanic rocks from Central Tibet: implications for the Central Asia inclination anomaly, the paleolatitude of Tibet and post-50 Ma shortening within Asia. Geophys. J. Int. 184, 131–146.
Liu, X.H., Ju, Y.T., Wei, L.J., Li, G.W., 2010. An alternative tectonic model for the Yarlung Zangbo Suture. Sci. China (Ser. D) 53 (1), 448–463.
Lowrie, W., 1990. Identification of ferromagnetic minerals in a rock coercivity and unblocking temperature properties. Geophys. Res. Lett. 17, 159–162.
McFadden, P.L., McElhinny, M.W., 1988. The combined analysis of remagnetization circles and direct observations in paleomagnetism. Earth Planet. Sci. Lett. 87, 161–172.
McFadden, P.L., 1990. A new fold test for paleomagnetic studies. Geophys. J. Int. 103, 163–169.
McFadden, P.L., McElhinny, M.W., 1990. Classification of the reversal test in palaeomagnetism. Geophys. J. Int. 103 (3), 725–729.
Mo, X.X., Niu, Y.L., Dong, G.C., Zhao, Z.D., Hou, Z.Q., Su, Z., Ke, S., 2008. Contribution of syncollisional felsic magmatism to continental crust growth: a case study of the Paleogene Linzizong volcanic succession in southern Tibet. Chem. Geol. 250, 49–67.
Mo, X.X., Zhao, Z.D., Deng, J.F., Dong, G.C., Zhou, S., Guo, T.Y., Zhang, S.Q., Wang, L.L., 2003. Response of volcanism to the India–Asia collision. Earth Sci. Front. 10, 135–148 (in Chinese).
Molnar, P., England, P., Martinod, J., 1993. Mantle dynamics, uplift of the Tibetan Plateau, and the Indian monsoon. Rev. Geophys. 31, 357–396.
Najman, Y., Appel, E., Boudagher-Fadel, M., et al., 2010. The timing of India–Asia collision: geological, biostratigraphic and palaeomagnetic constraints. J. Geophys. Res. 46, 531–554.
Ogg, J., Smith, A.G., 2004. The geomagnetic polarity time scale. In: Gradstein, F.M., Ogg, J.G., Smith, A.G. (Eds.), A Geological Time Scale. Cambridge University Press, Cambridge, Cambridge, pp. 63–86.
Owens, T.J., Zandt, G., 1997. Implications of crustal property variations for models of Tibetan plateau evolution. Nature 387, 37–43.
Pan, G.T., Ding, J., 2005. The Qinghai-Tibet Plateau and its adjacent area map 1:1500000. Chengdu Map Publishing House, Chengdu. China. (in Chinese).
Patriat, P., Achache, J., 1984. India Eurasia collision chronology has implications for crustal shortening and driving mechanism of plates. Nature 311, 615–621.
Patzelt, A., Li, H., Wang, J., Appel, E., 1996. Palaeomagnetism of Cretaceous to Tertiary sediments from southern Tibet: evidence for the extent of the northern margin of India prior to the collision with Eurasia. Tectonophysics 259, 259–284.
Qi, X.X., Zeng, L.S., Meng, X.J., Xu, Z.Q., Li, T.F., 2008. Zircon SHRIMP U–Pb dating for Dala granite in the Tethyan Himalaya and its geological implication. Acta Petrol. Sin. 24 (7), 1501–1508 (in Chinese).
Rage, J.C., 2003. Relationships of the Malagasy fauna during the late Cretaceous: northern or southern routes ? Acta Paleontol. Pol. 48, 661–662.
Ratschbacher, L., Frisch, W., Lui, G., Chen, C., 1994. Distributed deformation in southern Tibet during and after the India–Asia collision. J. Geophys. Res. 99 (B10), 19,917–19,945.
Raymo, M.E., Ruddiman, W.F., 1992. Tectonic forcing of late Cenozoic climate. Nature 359, 117–122.
Sahabi, M., 1993. Un modèl général de l'évolution de l'Océan Indien. Unpublished PhD thesis, Université Bretagne, Brest, p. 330.
Sun, Z., Jiang, W., Li, H., Pei, J., Zhu, Z., 2010. New paleomagnetic results of Paleocene volcanic rocks from the Lhasa block: tectonic implications for the collision of India and Asia. Tectonophysics 490, 257–266.
Tan, X., Gilder, S., Kodama, K.P., Jiang, W., Han, Y., Zhang, H., 2010. New paleomagnetic results from the Lhasa block: revised estimation of latitudinal shortening across Tibet and implications for dating the India–Asia collision. Earth Planet. Sci. Lett. 293, 396–404.
Tauxe, L., 2005. Inclination flattening and the geocentric axial dipole hypothesis. Earth Planet. Sci. Lett. 233, 247–261.
Tong, Y., Yang, Z., Zheng, L., Yang, T., Shi, L., Sun, Z., Pei, J., 2008. Early Paleocene paleomagnetic results from southern Tibet, and tectonic implications. Int. Geol. Rev. 50, 546–562.
Wan, X.Q., 1985. Cretaceous strata and foraminifera from Gamba, Tibet. Contributions to the geology of the Qinghai-Xizang (Tibet). Plateau 16, 203–228 (in Chinese).
Wan, X.Q., Zhao, W.J., Li, G.B., 2000. Restudy of the upper Cretaceous in Gamba, Tibet. Geoscience 14 (3), 281–285 (in Chinese).
Wan, X.Q., Jansa, L.F., Sarti, M., 2002a. Cretaceous and Paleogene boundary strata in southern Tibet and their implication for the India–Eurasia collision. Lethaia 35, 131–146.
Wan, X.Q., Liang, D.Y., Li, G.B., 2002b. Paleocene strata in Gamba, Tibet and influence of tectonism. Acta Geol. Sin. 76 (2), 155–162 (in Chinese).
Wang, J.G., Hu, X.M., Luba, J.S., Huang, Z.C., 2011. Provenance of the upper Cretaceous–Eocene deep-water sandstones in Sangdanlin, southern Tibet: constraints on the timing of initial India–Asia collision. J. Geol. 119 (3), 293–309.
Watson, G.S., Enkin, R.J., 1993. The fold test in paleomagnetism as a parameter estimation problem. Geophys. Res. Lett. 20, 2135–2137.
Wen, S.X., 1987a. Cretaceous system. Stratigraphy of the Mount Qomolangma Region. Science Press, Beijing, pp. 130–159 (in Chinese).
Wen, S.X., 1987b. Tertiary system. Stratigraphy of the Mount Qomolangma Region. Science Press, Beijing, pp. 160–180 (in Chinese).
Willems, H., Zhang, B.G., 1993. Cretaceous and lower Tertiary sediments of the Tethys Himalaya in the area of Gamba (south Tibet, PR China). In: Willems, H. (Ed.), Geoscientific Investigations in the Tethyan Himalayas: Ber. Fachbereich Geowiss. Univ. Bremen, 38, pp. 3–27.
Xu, Z.Q., Yang, J.S., Li, H.B., Zhang, Z.M., Liu, Y., 2011. On the tectonics of the India–Asia collision. Acta Geol. Sin. 85 (1), 1–33 (in Chinese).
Yin, A., Dubey, C.S., Kelty, T.K., Gehres, G.E., Chou, C.Y., Grove, M., Lovera, O., 2006. Structural evolution of the Arunachal Himalaya and implications for asymmetric development of the Himalayan orogen. Curr. Sci. 90, 195–206.
Yin, A., Dubey, C.S., Kelty, T.K., Webb, A.A.G., Harrison, T.M., Chou, C.Y., Célérier, J., 2010. Geologic correlation of the Himalayan orogen and Indian craton: part 2. Structural geology, geochronology, and tectonic evolution of the Eastern Himalaya. Geol. Soc. Am. Bull. 122 (3–4), 360–395.
Yin, A., Harrison, T.M., 2000. Geologic evolution of the Himalayan–Tibetan orogen. Annu. Rev. Earth Planet. Sci. Lett. 28, 211–280.
Zeng, L.S., Liu, J., Gao, L.E., Xie, K.J., Wen, L., 2009. Early Oligocene anatexis in the Yardoi gneiss dome, southern Tibet and geological implications. Chin. Sci. Bull. 54 (1), 104–112 (in Chinese).
Zhang, Z., Klemperer, S., 2010. Crustal structure of the Tethyan Himalaya, southern Tibet: new constraints from old wide-angle seismic data. Geophys. J. Int. 181, 1247–1260.
Zhao, W., Mechie, J., Brown, L.D., Guo, J., Haines, S., Hearn, T., Klemperer, S.L., Ma, Y.S., Meissner, R., Nelson, K.D., Ni, J.F., Pananont, P., Rapine, R., Ross, A., Saul, J., 2001. Crustal structure of central Tibet as derived from project INDEPTH wide-angle seismic data. Geophys. J. Int. 145, 486–498.
Zhao, W., Nelson, K.D., Che, J., Quo, J., Lu, D., Wu, C., Liu, X., 1993. Deep seismic reflection evidence for continental underthrusting beneath southern Tibet. Nature 366, 557–559.
Zijderveld, J.D.A., 1967. A.C. demagnetization of rocks: analysis of results. In: Collinson, D.W., Creer, K.M., Runcorn, S.K. (Eds.), Methods on Paleomagnetism. Elsevier, Amsterdam, pp. 254–286.